Precision Agriculture
https://doi.org/10.1007/s11119-022-09982-4

Using a low-cost unmanned aerial vehicle for mapping giant smutgrass in bahiagrass pastures

Gal Rozenberg[1,2] · **José Luiz C. S. Dias**[3] · **Wesley M. Anderson**[4] · **Brent A. Sellers**[5] · **Raoul K. Boughton**[6] · **Matheus B. Piccolo**[7] · **Lior Blank**[2]

Accepted: 12 December 2022

Abstract

Grasses within the *Sporobolus* genus have been classified as problematic weeds of pastures in many countries. In Florida, giant smutgrass is the most common and troublesome weedy *Sporobolus* grass. The use of unmanned aerial vehicles (UAVs) for mapping, combined with site-specific weed control has the potential to optimize giant smutgrass management and decrease the use of herbicides. In this research, RGB ortho-mosaics captured from a simple UAV were examined to detect and map giant smutgrass in bahiagrass pastures in Florida. Two sampling dates (May and August) and four flight altitudes (50, 75, 100 and 120 m) were investigated for optimal classification accuracy. Spectral, texture and combined (spectral and texture) analyses served as the basis for supervised (random forest) and unsupervised (k means) classifications. Giant smutgrass cover was successfully mapped and best evaluated by integrating the combined analysis with supervised algorithm, reaching a correlation of 0.91 with the ground truth cover. Flight altitude had a negative relationship with giant smutgrass detection; however, satisfactory results were also obtained from 120 m with an average correlation of 0.76 when using combined supervised classification. Additionally, both sampling dates were found adequate for giant smutgrass mapping. These findings demonstrate that low-cost UAV platforms can successfully be used to generate accurate giant smutgrass infestations maps, allowing for site-specific management in bahiagrass pastures. Results from this work also broaden the general knowledge on the impacts that different settings and parameters (e.g. time of the year, altitude and image-analyses methods) can have on aerial image classification.

Keywords Classification · Drone · Site-specific weed management · Weed detection

Introduction

Weedy *Sporobolus* grasses are invasive perennial warm-season bunch grasses believed to be native to tropical Asia (Wunderlin & Hansen, 2003). They have been widely recognized as problematic weeds in pasture systems throughout the world (Dias-Filho, 2015;

✉ José Luiz C. S. Dias
joseluizdias@arizona.edu

Extended author information available on the last page of the article

Palmer, 2012), including the southeastern United States (Ferrell et al., 2006; Mislevy et al., 2002; Rana et al., 2015). In Florida, the spread of giant smutgrass (*Sporobolus indicus* var. *pyramidalis*) in bahiagrass pastures (*Paspalum notatum*) is of growing concern. Giant smutgrass is a prolific seed producer (Currey et al., 1973) that can quickly spread to new areas, resulting in significant reductions in forage production (Ferrell et al., 2006). Additionally, selective over-the-top herbicides are limited and expensive, making effective and economic viable long-term management very difficult to achieve (Sellers et al., 2018).

An emerging approach to reduce the overall use and cost of herbicides is site-specific weed management (SSWM). Traditionally, herbicides are applied uniformly across fields; nonetheless, weeds tend to aggregate in patches rather than being uniformly distributed (Blank et al., 2019; Rozenberg et al., 2021). Accordingly, SSWM utilizes the weeds clustered spatial pattern to perform customized site-specific spraying, accounting for both weed location and infestation level, thereby decreasing the excessive use of chemicals, expenses (Nordmeyer, 2006), chances of crop injury, as well as off-target movement potential.

One of the critical components and challenges for SSWM implementation is weed monitoring and the ability to generate quick, accurate and precise weed maps. While traditional in-person field scouting is labor-intensive, costly and likely not feasible for large-scale settings, remote sensing via unmanned aerial vehicles (UAVs) offers an exceptional solution (Huang et al., 2018). The use of UAV platforms for photogrammetry has several advantages including the ability to fly at low altitudes, allowing for greater spatial resolution imagery and for the possibility to identify small individual plants and/or weed patches (Xiang & Tian, 2011). However, there is an inherent trade-off between area coverage, flight altitude and UAV flight time. An optimized flight altitude will allow for large area coverage while obtaining satisfactory resolution allowing weed detection (Borra-Serrano et al., 2015).

There is a possible complication in the detection and mapping of weeds due to their shared visual characteristics with crops. When possible, e.g., in crop rows, one can incorporate spatial information of a plant location in the classification process to discriminate crop from weeds (Louargant et al., 2018). However, this type of analysis cannot be carried out on pastures because they have homogeneous coverage. Alternatively, spectral-based classification derived from phenological differences among weeds and crops has been suggested and served as the basis for weed mapping via remote sensing (Castillejo-González et al., 2014; Lamb & Brown, 2001; Rasmussen et al., 2018; Rozenberg et al., 2021). Utilizing phenological differences of weed and crop to distinguish between the two should consider the time within the season for image acquisition to maximize the spectral contrast (López-Granados et al., 2010). Additionally, attributes such as height (Zisi et al., 2018), texture (Yuba et al., 2021) and shape (Bakhshipour & Jafari, 2018) should also be considered as they may contribute to classification accuracy.

Numerous classification algorithms have been utilized for weed mapping, each with its own advantages and drawbacks (Mohidem et al., 2021). An automated classification procedure is likely to avoid errors that may derive from human input introduced into the process (de Castro et al., 2018) and facilitate the implementation of weed mapping using UAVs by inexperienced end-users (Gašparović et al., 2020). However, a fully automated weed mapping process remains a challenge (Mohidem et al., 2021), even in well-defined spectral differences (Rasmussen et al., 2018). While the latest state-of-the-art classification algorithms such as deep neural networks hold promising results, they require computational power and large training datasets (Bakhshipour & Jafari, 2018; Mohidem et al., 2021). Alternatively, classification of weeds has been accomplished by relatively simple methods (e.g., Gašparović et al., 2020; Rozenberg et al., 2021). Integrating imagery produced from low-cost UAV with open source relatively simple procedures may allow for economic and rapid weed map generation for site-specific management.

In order to optimize the use of UAVs for weed mapping it is important to determine the ideal parameters for imagery acquisition as well as the effectiveness of the image analysis algorithms and weed mapping approach. Therefore, the objectives of this study were to determine the effects of flight altitude and time of imagery acquisition during the season on the effectiveness of giant smutgrass mapping in bahiagrass pastures. Additional objective was to compare methods to classify and detect weeds, by using both supervised and unsupervised classification algorithms. It is hypothesized that the increases in flight altitude are likely to negatively affect giant smutgrass detection accuracy due to loss of spatial and spectral resolution. Furthermore, classification accuracy is expected to be higher in the summer due to the more evident phenological differences and consequently spectral contrast between giant smutgrass and bahiagrass.

Material and methods

Experimental site

This work was conducted at the University of Florida Institute of Food and Agricultural Sciences (UF/IFAS) Range Cattle Research and Education Center, near Ona, FL, in 2017. Two research sites (27° 22.8′ N 81° 56.64′ W and 27° 23.52′ N 81° 57′ W) of 105 × 105 m (~ 1.1 ha) were delimitated in two established bahiagrass pastures naturally infested with giant smutgrass (Fig. 1). The two pastures were being continuously stocked during the study and were selected based on their different levels of giant smutgrass infestation. Giant smutgrass infestation was visually estimated to be 20–30% and 60–70% of ground cover for the Low Field (LF) and High Field (HF), respectively. Both fields were sampled in early May and early August in 2017. The sampling dates were chosen to represent the dry (May) and wet (August) seasons (Table 1).

Acquisition of aerial photographs and field sampling

The DJI Phantom 4 (SZ DJI Technology Co., Ltd., Shenzen, Guangdong, China), a popular recreational UAV platform with vertical take-off and landing (VTOL), was employed to acquire digital images within the two study sites. This UAV had an integrated RGB camera, acquires 1-inch 20-megapixels images in true color (Red, R; Green, G; and Blue, B, bands) and has an optimized f/2.8 wide-angle lens. The camera's sensor is a 25 mm complementary metal-oxide semiconductor (CMOS) with 20 M effective pixels.

The UAV was employed at the LF and HF locations, at four different flights altitudes (50, 75, 100 and 120 m). Flights were conducted at a maximum speed of 5 m/s with a frontal and side image overlap of 75%. Simultaneously to the UAV flights, a systematic and on-ground sampling procedure was carried out. In each field, 56 sampling quadrats of 1.5 × 1.5 m were placed in a grid-like shape, placing a quadrat every 15 m throughout the study area surface. Each quadrat was georeferenced with a Trimble GeoExplorer 6000 series GeoXH (Trimble Inc, Sunnyvale, California, USA), and giant smutgrass percent cover was visually estimated on-ground on the same days that the images were acquired. All ground cover estimates were performed by a single observer to ensure uniformity and

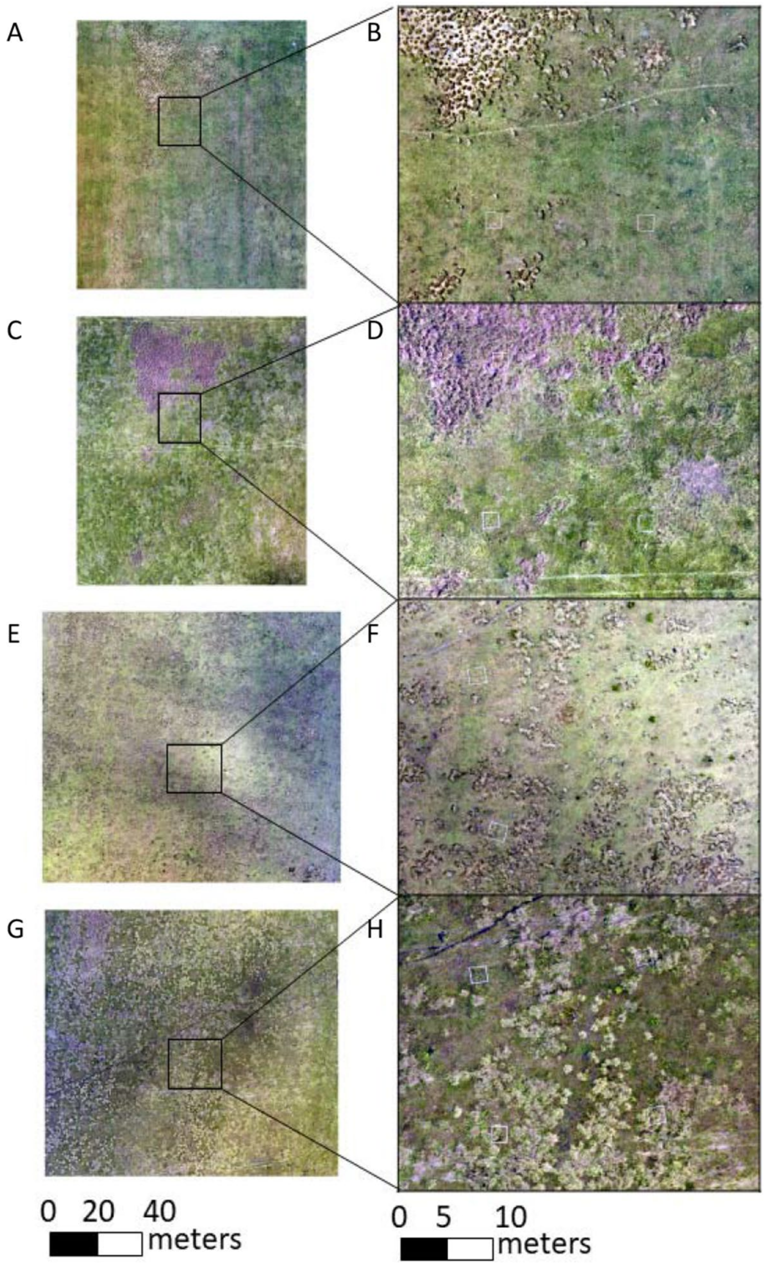

Fig. 1 Ortho-mosaics acquired at an altitude of 50 m for the entire research area of LF pasture in May and August (**A** and **C**, respectively) along with area zoom-in (**B** and **D**, respectively) and for the HF pasture in May and August (**E** and **G**, respectively) with corresponding zoom-in example (**F** and **H**, respectively)

Table 1 Average temperature and monthly precipitation obtained in sampling months from the UF/IFAS weather station at the Range Cattle Research and Education Center

Month	Precipitation (mm)	Temperature (C°)
May	64	25
August	272	27

to avoid subjective variability. In addition, six artificial terrestrial targets (ATTs) were used to perform the imagery ortho-rectification and mosaicking process.

Imagery was collected in digital negative (DNG) format. Upon flight completion, all imagery was converted to JPEG using Photoshop CC 2018 v. 19.1.4 (Adobe Inc., San Jose, CA, USA). Converted images from each flight were mosaicked into a single image using the online browser-based service Maps Made Easy (Drones Made Easy, San Diego, CA, USA). Although other platforms are available for mosaicking imagery, such as ArcGIS and Drone Deploy, Maps Made Easy was the most economical for this study.

Image classification and validation

The image classification procedure was constructed in two steps: analysis and classification. First, the RGB ortho-mosaic was analyzed to obtain meaningful spectral and textural layers. An additional combined analysis was comprised of both initial analyses. Second, the layers produced were used to detect giant smutgrass employing two classification algorithms (Fig. 2).

Due to the giant Smutgrass phenology i.e., brown seedheads, which may contrast with the green bahiagrass, spectral-based classification was initially examined using a vegetation index. Considering that the RGB camera captures images within the visible-spectrum, vegetation indices based on the relation between the red, green and blue

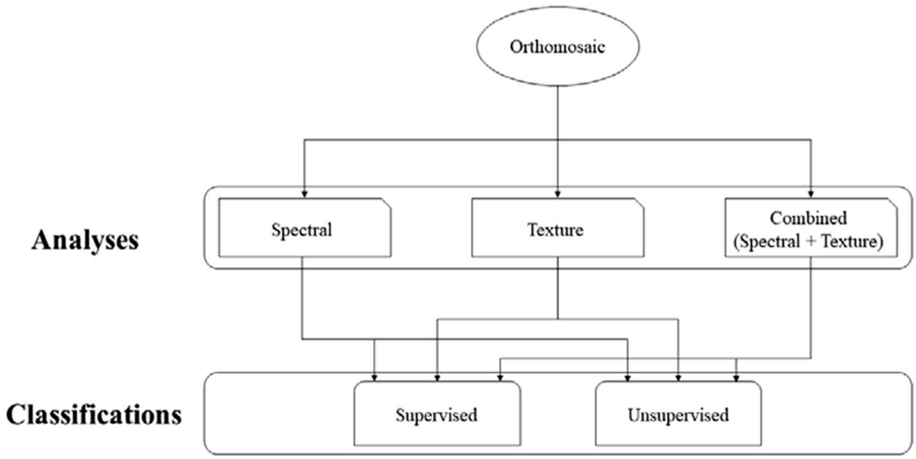

Fig. 2 Simplified scheme of the two-step classification procedure. First, the three analyses were performed on the ortho-mosaics. Second, the produced layers served as the basis for the two-classification algorithm utilized

channels, are commonly used to emphasize plant material. Based on preliminary examinations the color index of vegetation extraction (CIVE), was adopted (Kataoka et al., 2003; Eq. 1).

$$CIVE = (0.441 * R) - (0.811 * G) + (0.385 * B) \tag{1}$$

where $R = \frac{r}{r+g+b}$, $G = \frac{g}{r+g+b}$ and $B = \frac{b}{r+g+b}$. The parameters r, g and b are normalized values between 0 and 1 expressed as: $r = \frac{red}{red_{max}}$, $g = \frac{green}{green_{max}}$ and $b = \frac{blue}{blue_{max}}$ where *red green* and *blue* are the original pixel values and red_{max}, $green_{max}$ and $blue_{max}$ all equal 255 and are the maximum value of their respected spectral channel.

Texture analysis may unveil patterns that are not captured within the spectral realm and thereby increase classification accuracy. Second-order textures, used in this research, measure the probability of each pair of pixels co-occurring within a specified distance and direction (Haralick et al., 1973). Texture analysis was carried out using the gray-level co-occurrence Matrix (GLCM) package in R (Zvoleff, 2020). The 'glcm' function generates eight second-order texture-based rasters: mean, variance, contrast, correlation, homogeneity, dissimilarity, entropy and second moment. Further explanation and texture equations can be found in Haralick et al. (1973). Each of these eight indices is calculated per pixel located at the center of a moving window size that contains a number of rows and columns of pixels specified by the user. Texture analysis may be influenced by the selected window size (Feng et al., 2015). Following a careful examination and preliminary analyses, two indices, the homogeneity and entropy layers produced with a 5×5 window size, were chosen to represent the texture analysis. Finally, the homogeneity and entropy layers were coupled with the vegetation index layer to create a raster comprised of both texture and spectral characteristics.

All three analyses, i.e., spectral, texture and the combined analyses, were employed to classify each ortho-mosaic using both supervised and unsupervised classification. For the first, the random forest algorithm was employed. Random forest is a cutting-edge machine learning algorithm applied to supervised classification that has recently been used successfully to classify weeds in various conditions (e.g., de Castro et al., 2018; Gao et al., 2018; Yuba et al., 2021). Supervised classification requires user input of training samples. Overall, twelve training samples, depicted as polygons, were constructed to represent the two classes – "*giant smutgrass*" and "*other*", six polygons for each class. The polygons varied in size but were identical between the two groups i.e. the same polygon sizes and shapes were used in both classes. The highest resolution ortho-mosaic (50 m flight altitude) was utilized to delimit these polygons. However, the training process of each classification was done to each ortho-mosaic separately. In contrast, user input is not necessary for the unsupervised classification, and k-means algorithm was employed by simply setting the number of classes to two. The random forest and k-means algorithms were employed using the '*superClass*' and '*unsuperClass*' functions, respectively, in the RSToolbox package (Leutner et al., 2019). Finally, a majority filter was applied to reduce "salt-and-pepper" effect, where pixel values were altered according to their neighbors as utilized in previous research (Lu & Weng, 2007; Rozenberg et al., 2021).

Based on the classification maps, giant smutgrass cover was calculated within the 56 ground truth quadrats as the percentage of pixels classified as giant smutgrass out of the total pixels in each quadrat. Giant smutgrass calculated from the classification maps was tested for correlation with the ground truth visual cover in each quadrat estimated in the field. All the analyses were performed using R studio 1.1.456 (R Development Core Team, Vienna, Austria).

Results

In total, sixteen ortho-mosaics were produced. The two pastures were surveyed at two sampling dates from four different flight altitudes. For each ortho-mosaic, six weed maps were generated. Spectral-, texture- and combined (spectral and texture) -based analyses were examined by employing supervised and unsupervised classification.

By integrating the correlations to the ground truth visual cover from all flight altitudes, it was found that the spectral analysis was insufficient using both supervised and unsupervised classifications in the HF pasture (average R correlation = 0.46), but the texture and combined analyses performed well using both classification algorithms (Fig. 3). The texture analysis followed by supervised classification obtained high correlations in the LF pasture in May (average R correlation = 0.77), whereas spectral analysis outperformed the texture analysis in August with average R correlation of 0.76 and 0.55, respectively; however, the texture analysis correlations were less consistent. The combined analysis performed well for both sampling dates using the supervised classification reaching a correlation of 0.91 with low variability, indicating satisfactory and reliable results (Fig. 3).

In the next step, the effect of flight altitude on classification performance was examined. For that, correlations to the ground truth visual cover of the two sampling months, for both LF and HF, were combined. Supervised classification outperformed unsupervised classification at all flight altitudes (Fig. 4). For the combined supervised classification, the highest correlation of giant smutgrass detection with the ground truth estimations was produced from the lowest flight altitudes, i.e., 50 m with average R correlation of 0.85 (Fig. 4). Correlations acquired from altitudes of 75 m and 100 m were similar though, for the supervised classification, greater variability was found at 100 m. The lowest correlations were at a flight altitude of 120 m (average R correlation = 0.76). The effect of flight altitude on classification accuracy was affected by the sampling date. While, in May, the correlation was similar across all four flight altitudes, in August, the correlation decreased as altitude increased (Fig. 5).

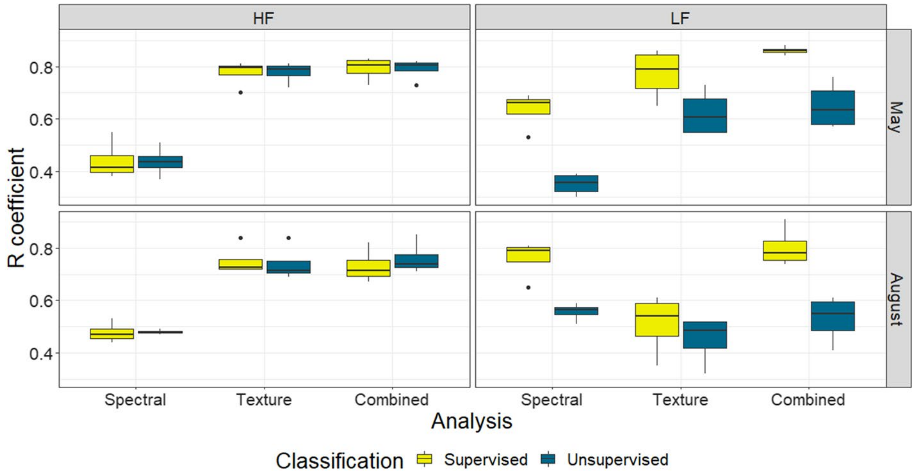

Fig. 3 Correlations between giant smutgrass cover field estimations (ground truth) and cover calculated from classifications maps considering the two research fields at both sampling dates

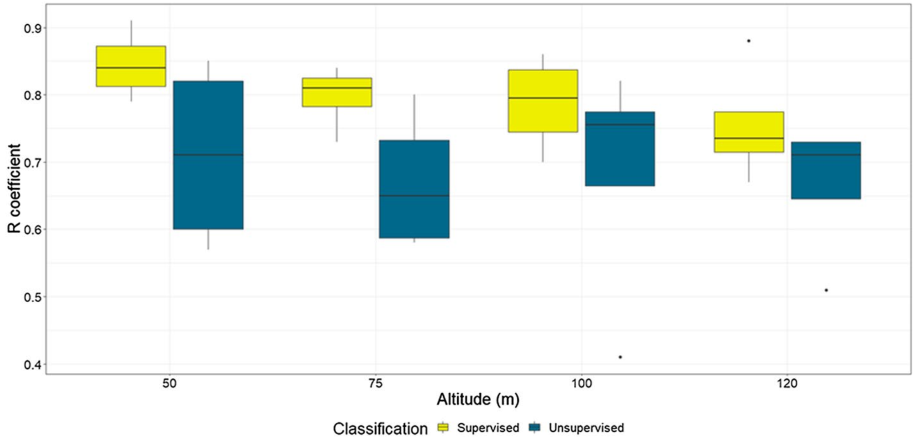

Fig. 4 Correlations of giant smutgrass cover field estimations and cover calculated from classifications maps based on the combined analysis

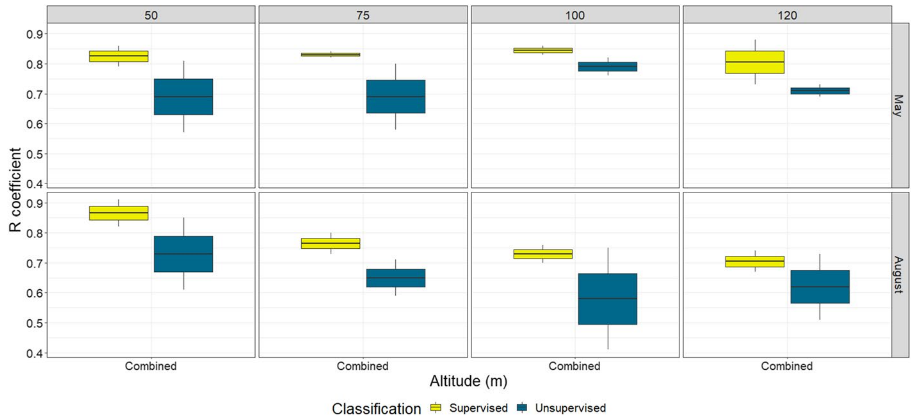

Fig. 5 Correlations of giant smutgrass cover field estimations and cover calculated from classifications maps based on the combined analysis considering altitude and sampling date

Finally, weed maps with the highest correlation were used to calculate total smutgrass coverage in each field and date. For three out of the four cases (HF in May and LF in both dates), combined analysis with supervised classification produced the highest correlations. For HF in August, the combined analysis followed by the unsupervised classification performed slightly better (R = 0.85) than the supervised classification (R = 0.82). For the LF pasture, giant smutgrass coverage was 16.8% in May and 14.6% in August. In the HF pasture, giant smutgrass coverage was 44.1% and 52.9% for May and August, respectively (Fig. 6).

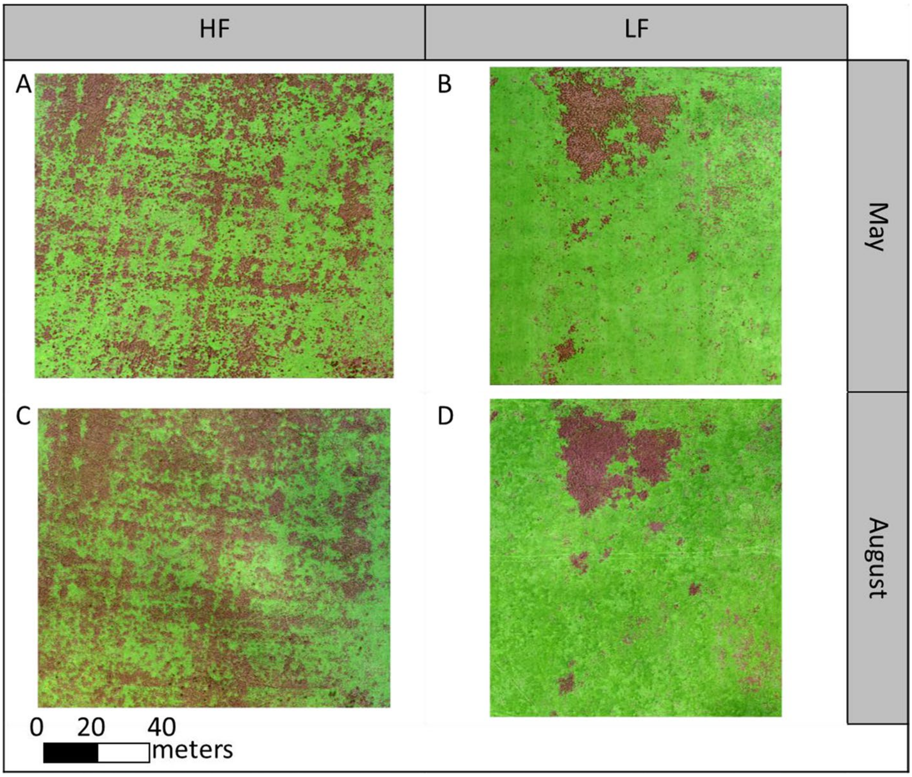

Fig. 6 Classification maps with the highest correlation were produced for HF and LF pastures in May (**A** and **B**, respectively) and August (**C** and **D**, respectively). Brown represents giant smutgrass, and green represents other surface cover e.g., soil or bahiagrass

Discussion

Examining various combinations of image analysis and classification methods resulted in successful mapping of giant smutgrass. Despite the expected phenological differences between giant smutgrass and bahiagrass, classification based solely on spectral differences was not sufficient. As an alternative, textural and combined texture-spectral based classifications were used to improve weed detection. Similar techniques were employed to map different weed species in previous studies when spectral differences were not sufficient either by using RGB camera (Yuba et al., 2021) or advanced cameras, i.e. multispectral images (Tamouridou et al., 2017; Zisi et al., 2018). In this research, texture analysis alone yielded satisfactory results for three out of four cases whereas, when combined with the spectral input, it improved the correlation with the ground truth data for each of the analyses.

Image classification

Giant smutgrass was successfully classified in the two research fields and at two sampling dates employing the combined analysis with supervised classification. However, the contribution of spectral and texture information to the classification success varied. In the HF pasture, the texture analysis consistently acquired high correlation. In the LF pasture, the spectral and texture analyses resulted in contrasting success between the two sampling dates. Several factors may contribute to the contrasting analyses projected on the classification accuracies in the different cases: bahiagrass vigor, the development of giant smutgrass seedheads and the grazing intensity. The HF pasture was not only characterized by a high infestation rate of giant smutgrass but also by degraded bahiagrass conditions and more bare ground areas lacking any vegetative cover. Several factors may have contributed to the degraded bahiagrass conditions and bare ground areas in the HF field, including the lower nutritive value of giant smutgrass, which results in bahiagrass being overgrazed (Wilder et al., 2011), feral swine rooting, as well as lack of proper adoption of recommended agronomic practices such as liming and fertilizer applications. Consequently, brown soil patches were noticeable and shared a similar spectral signature to the giant smutgrass. The process was further complicated when, due to the absence of desirable forage availability, the animals may graze the giant smutgrass plants, resulting in fewer seedheads and new tissue growth, i.e., green material that shares spectral attributes with the bahiagrass.

Overall, the supervised classification yielded good and reliable results across all cases in this research. The unsupervised classification yielded satisfactory and comparable results to the supervised classification for the HF field, whereas the supervised classification outperformed the unsupervised classification in the LF area. There are known limitations to both supervised and unsupervised methods for classifying remotely sensed images. In general, supervised classification algorithms tend to be more computationally intensive, require a considerable amount of preparation time, and are hard to reproduce, whereas unsupervised algorithms tend to have lower accuracy because a priori knowledge about the study area is not included in the process.

Time of imagery acquisition during the season

Similar setting found in HL (i.e. bahiagrass vigor, vegetative cover) was found for the LF pasture area in May. Therefore, spectral-based classification performed poorly in those cases. However, for the LF pasture in August, when the season progressed and rain began to support the pasture, the improved condition of the bahiagrass resulted in better coverage of the soil and green non-stressed bahiagrass along with the growth of brownish giant smutgrass seedheads allowed for fine spectral discrimination. In contrast, actively growing bahiagrass patches exhibited similar textural characteristics to the giant smutgrass resulting in relatively low accuracy scores of the corresponding analysis at this time. Finally, satisfactory accuracy scores were acquired at the two sampling dates when the combined analysis was used; thus, both May and August were found adequate for combined analysis-based giant smutgrass mapping. This is an important finding for two reasons. First, a known problem with image classifications methods is that they are context-specific (Mohidem et al., 2021). Nonetheless, the combined analysis was robust for the two fields and two sampling dates. Secondly, accurately mapping giant smutgrass at different times of the year gives ranchers more flexibility to plan their giant smutgrass management program. For example, May mappings could be readily used if the goal is to control giant smutgrass with the selective but expensive herbicide hexazinone since this herbicide has been shown to be more effective in July (Dias, 2019). Conversely, August mappings could be used if the goal is to manage giant smutgrass with cheaper but non-selective herbicide options such as glyphosate, which tends to be more effective when applied in September (Davy et al., 2012).

Flight altitude

Low flight altitudes allow higher spatial and spectral resolution, whereas high altitudes allow UAV to cover a larger area and decrease image processing time (Borra-Serrano et al., 2015). Previous studies reported that reduced spatial resolution of the ortho-mosaic had little to no adverse effect on classification accuracy (Rasmussen et al., 2018; Rozenberg et al., 2021; Tamouridou et al., 2017). Pérez-Ortiz et al. (2015), reported similar classification results from 30 to 60 m yet the accuracy decreased when flight altitude increased to 100 m. While mapping *Pennisetum alopecuoides* in grazed pastures, Yuba et al. (2021) examined four altitudes comparable to some extent to the altitudes examined in this research and achieved high accuracies across all altitudes. Yet, the highest accuracy corresponded to the highest spatial resolution, i.e., the lowest flight altitude of 28 m. Overall, these findings are consistent with the results found in this research although the lowest altitude here was 50 m. On average, the highest correlations were obtained upon comparing ground truth estimations with classification maps acquired at the lowest altitude. However, high correlations were also found for increased flight altitudes, including the highest flight of 120 m, especially for images acquired in May. Therefore, if the mapping of a large area is needed, it is possible to increase the UAV flight altitude and still acquire satisfactory giant smutgrass weed maps.

Implications for weed management

The two research locations displayed different infestation levels. Considering herbicide costs and possible negative effects on bahiagrass, Ferrell et al. (2006) recommended broadcast applications of hexazinone at 1.12 kg ai ha^{-1} only after giant smutgrass cover exceeds 35%. One direct and readily available benefit of the generation of giant smutgrass infestation maps, by adopting methods proposed in this work, would be the identification of giant smutgrass infested fields that meet these requirements. For example, the HF pasture (in both sampling dates) is qualified for positive return of investment broadcast applications of hexazinone. Another benefit of generating giant smutgrass infestation maps is the possibility to manage pastures before the economic thresholds of giant smutgrass infestation (35% groundcover) are reached by employing SSWM. Site-specific giant smutgrass management can therefore decrease the detrimental impacts of giant smutgrass interference even in low-infested fields, optimizing forage production and quality (Ghanizadeh & Harrington, 2019), while at the same time slowing giant smutgrass expansion rate within the same field, as well as to non-infested fields. Likewise, SSWM may allow the use of other non-selective herbicides such as glyphosate to manage giant smutgrass in bahiagrass pastures since only the giant smutgrass plants would be sprayed. Furthermore, it is important to note that giant smutgrass is a perennial species which were generally reported to be stable in their location across years (Blank et al., 2019; Colbach et al., 2000). Therefore, the mapping of one year may be used for weed management in the following year (Lati et al., 2022). However, this still needs further investigations and might vary based on the type of bahiagrass grazing management program.

In recent years, a large and growing body of literature has examined the application of UAVs for numerous environmental observations (Manfreda et al., 2018). Ease-of-use, flexibility and high spatial resolution images are merely a subset of the UAVs qualities to make them suitable for precision agriculture (Hunt & Daughtry, 2018) and particularly for precise weed management (Huang et al., 2018; Mohidem et al., 2021). UAVs have been reported to facilitate various monitoring aspects in pastures, e.g., biomass (Batistoti et al., 2019) and quality (Barnetson et al., 2020). Therefore, a single flight campaign may potentially provide diverse information to facilitate knowledge-based decisions in pasture management.

Conclusions

In this study, classification based exclusively on spectral or textural analyses was not sufficient. However, integrating the two methods improved classification accuracy. Although flight altitude negatively impacted giant smutgrass detection, satisfactory results allowing weed detection, were also obtained at the highest flight altitude (120 m). In addition, discrimination of smutgrass can be accomplished in both May and August, which means that applying SSWM to both dates is possible. In conclusion, giant smutgrass can be accurately mapped based on ortho-mosaics produced from RGB images captured using a low-cost UAV.

Acknowledgements The authors would like to acknowledge all the graduate research students and interns from the UF-IFAS Range Cattle Research and Education center that helped with all field work during image and giant smutgrass cover data acquisition.

Data availability Not applicable.

Declarations

Conflict of interest The authors declare that they have no conflict of interest.

References

Bakhshipour, A., & Jafari, A. (2018). Evaluation of support vector machine and artificial neural networks in weed detection using shape features. *Computers and Electronics in Agriculture, 145*, 153–160. https://doi.org/10.1016/j.compag.2017.12.032

Barnetson, J., Phinn, S., & Scarth, P. (2020). Estimating plant pasture biomass and quality from UAV Imaging across Queensland's Rangelands. *AgriEngineering, 2*(4), 523–543. https://doi.org/10.3390/agriengineering2040035

Batistoti, J., Marcato Junior, J., Ítavo, L., Matsubara, E., Gomes, E., Oliveira, B., et al. (2019). Estimating pasture biomass and canopy height in Brazilian Savanna using UAV photogrammetry. *Remote Sensing, 11*(20), 2447. https://doi.org/10.3390/rs11202447

Blank, L., Birger, N., & Eizenberg, H. (2019). Spatial and temporal distribution of *Ecballium elaterium* in Almond orchards. *Agronomy, 9*(11), 751–751. https://doi.org/10.3390/agronomy9110751

Borra-Serrano, I., Peña, J. M., Torres-Sánchez, J., Mesas-Carrascosa, F. J., & López-Granados, F. (2015). Spatial quality evaluation of resampled unmanned aerial vehicle-imagery for weed mapping. *Sensors, 15*(8), 19688–19708. https://doi.org/10.3390/s150819688

Castillejo-González, I. L., Peña-Barragán, J. M., Jurado-Expósito, M., Mesas-Carrascosa, F. J., & López-Granados, F. (2014). Evaluation of pixel- and object-based approaches for mapping wild oat (*Avena sterilis*) weed patches in wheat fields using QuickBird imagery for site-specific management. *European Journal of Agronomy, 59*, 57–66. https://doi.org/10.1016/j.eja.2014.05.009

Colbach, N., Forcella, F., & Johnson, G. A. (2000). Spatial and temporal stability of weed populations over five years. *Weed Science, 48*(3), 366–377. https://doi.org/10.1614/0043-1745(2000)048[0366:satsow]2.0.co;2

Currey, W. L., Parrado, R., & Jones, D. W. (1973). Seed characteristics of smutgrass (*Sporobolus poiretii*). In *Proceedings of the 32nd Soil Crop Science Society of Florida* (pp. 53–54). Gainesville, FL, USA: Soil and Crop Science Society of Florida.

Davy, J., Forero, L., Nader, G., Ditomaso, J., & Kyser, G. (2012). *Managing smutgrass in irrigated pastures*. California, USA: University of California, Agriculture and Natural Resources. https://doi.org/10.3733/ucanr.8473

de Castro, A. I., Torres-Sánchez, J., Peña, J. M., Jiménez-Brenes, F. M., Csillik, O., & López-Granados, F. (2018). An automatic random forest-OBIA algorithm for early weed mapping between and within crop rows using UAV imagery. *Remote Sensing, 10*(2), 285. https://doi.org/10.3390/rs10020285

Dias J. L. C. (2019). Implementation of integrated strategies to manage giant smutgrass (*sporobolus indicus var. Pyramidalis*) infestations in bahiagrass pastures. PhD Dissertation, University of Florida, Gainesville, FL, USA

Dias-Filho MB (2015). Formação e manejo de pastagens. Belém, PA: Embrapa Amazônia Oriental. "Management and establishment of pasture. Belém, PA: Eastern Amazon Embrapa." Retrieved [April 2019] from https://www.infoteca.cnptia.embrapa.br/infoteca/handle/doc/937485.

Feng, Q., Liu, J., & Gong, J. (2015). UAV Remote sensing for urban vegetation mapping using random forest and texture analysis. *Remote Sensing, 7*(1), 1074–1094. https://doi.org/10.3390/rs70101074

Ferrell, J. A., Mullahey, J. J., Dusky, J. A., & Roka, F. M. (2006). Competition of giant Smutgrass (*Sporobolus indicus*) in a Bahiagrass pasture. *Weed Science, 54*(1), 100–105.

Gao, J., Liao, W., Nuyttens, D., Lootens, P., Vangeyte, J., Pižurica, A., et al. (2018). Fusion of pixel and object-based features for weed mapping using unmanned aerial vehicle imagery. *International Journal of Applied Earth Observation and Geoinformation, 67*, 43–53. https://doi.org/10.1016/j.jag.2017.12.012

Gašparović, M., Zrinjski, M., Barković, Đ, & Radočaj, D. (2020). An automatic method for weed mapping in oat fields based on UAV imagery. *Computers and Electronics in Agriculture, 173*, 105385. https://doi.org/10.1016/j.compag.2020.105385

Ghanizadeh, H., & Harrington, K. C. (2019). Weed management in New Zealand pastures. *Agronomy, 9*(8), 448. https://doi.org/10.3390/agronomy9080448

Haralick, R. M., Shanmugam, K., & Dinstein, I. (1973). Textural features for image classification. *IEEE Transactions on Systems, Man, and Cybernetics, 3*(6), 610–621. https://doi.org/10.1109/TSMC.1973.4309314

Huang, Y., Reddy, K. N., Fletcher, R. S., & Pennington, D. (2018). UAV low-altitude remote sensing for precision weed management. *Weed Technology, 32*(1), 2–6. https://doi.org/10.1017/wet.2017.89

Hunt, E. R., & Daughtry, C. S. T. (2018). What good are unmanned aircraft systems for agricultural remote sensing and precision agriculture? *International Journal of Remote Sensing, 39*(15–16), 5345–5376. https://doi.org/10.1080/01431161.2017.1410300

Kataoka, T., Kaneko, T., Okamoto, H., & Hata, S. (2003). Crop growth estimation system using machine vision. In *Proceedings 2003 IEEE/ASME International Conference on Advanced Intelligent Mechatronics* (pp. b1079–b1083). Kobe, Japan: IEEE. https://doi.org/10.1109/AIM.2003.1225492

Lamb, D. W., & Brown, R. B. (2001). Remote-sensing and mapping of weeds in crops. *Journal of Agricultural Engineering Research, 78*(2), 117–125. https://doi.org/10.1006/JAER.2000.0630

Lati, R. N., Gerhards, R., Eizenberg, H., Matzrafi, M., Blank, L., & Christensen, S. (2022) Advances in precision application technologies for weed management. In Kudsk, P. (Ed.), Advances in integrated weed management. Cambridge, UK: Burleigh Dodds Publishing.

Leutner, B., Horning, N., Schwalb-Willmann, J., & Hijmans, R. J. (2019). *RStoolbox: Tools for remote sensing data analysis*. Retrieved July 25, 2021, from https://CRAN.R-project.org/package=RStoolbox.

López-Granados, F., Gómez-Casero, M. T., Peña-Barragán, J. M., Jurado-Expósito, M., & García-Torres, L. (2010). Classifying irrigated crops as affected by phenological stage using discriminant analysis and neural networks. *Journal of the American Society for Horticultural Science, 135*(5), 465–473.

Louargant, M., Jones, G., Faroux, R., Paoli, J.-N., Maillot, T., Gée, C., et al. (2018). unsupervised classification algorithm for early weed detection in row-crops by combining spatial and spectral information. *Remote Sensing, 10*(5), 761–761. https://doi.org/10.3390/rs10050761

Lu, D., & Weng, Q. (2007). A survey of image classification methods and techniques for improving classification performance. *International Journal of Remote Sensing, 28*(5), 823–870. https://doi.org/10.1080/01431160600746456

Manfreda, S., McCabe, M., Miller, P., Lucas, R., Pajuelo Madrigal, V., Mallinis, G., et al. (2018). On the use of unmanned aerial systems for environmental monitoring. *Remote Sensing, 10*(4), 641–641. https://doi.org/10.3390/rs10040641

Mislevy, P., Martin, F. G., & Hall, D. W. (2002). West Indian dropseed/giant smutgrass (*Sporobolus indicus* var. pyramidalis) control in Bahiagrass (*Paspalum notatum*) pastures. *Weed Technology, 16*(4), 707–711. https://doi.org/10.1614/0890-037X(2002)016[0707:WIDGSS]2.0.CO;2

Mohidem, N. A., Che'Ya, N. N., Juraimi, A. S., Fazlil Ilahi, W. F., Mohd Roslim, M. H., Sulaiman, N., et al. (2021). How can unmanned aerial vehicles be used for detecting weeds in agricultural fields? *Agriculture, 11*(10), 1004. https://doi.org/10.3390/agriculture11101004

Nordmeyer, H. (2006). Patchy weed distribution and site-specific weed control in winter cereals. *Precision Agriculture, 7*(3), 219–231. https://doi.org/10.1007/s11119-006-9015-8

Palmer, W. A. (2012). Sporobolus spp. - weedy sporobolus grasses. In M. Julien, R. McFadyen, & J. Cullen (Eds.), (pp. 569–575). Melbourne, Australia: CSIRO Publishing.

Pérez-Ortiz, M., Peña, J. M., Peña, P., Gutiérrez, P. A., Torres-Sánchez, J., Hervás-Martínez, C., et al. (2015). A semi-supervised system for weed mapping in sunflower crops using unmanned aerial vehicles and a crop row detection method. *Applied Soft Computing Journal, 37*, 533–544. https://doi.org/10.1016/j.asoc.2015.08.027

Rana, N., Sellers, B. A., Ferrell, J. A., MacDonald, G. E., Silveira, M. L., & Vendramini, J. M. (2015). Integrated management techniques for long-term control of giant smutgrass (*Sporobolus indicus* var. pyramidalis) in Bahiagrass pasture in Florida. *Weed Technology, 29*(3), 570–577. https://doi.org/10.1614/WT-D-15-00021.1

Rasmussen, J., Nielsen, J., Streibig, J. C., Jensen, J. E., Pedersen, K. S., & Olsen, S. I. (2018). Pre-harvest weed mapping of *Cirsium arvense* in wheat and barley with off-the-shelf UAVs. *Precision Agriculture, 20*(5), 983–999. https://doi.org/10.1007/s11119-018-09625-7

Rozenberg, G., Kent, R., & Blank, L. (2021). Consumer-grade UAV utilized for detecting and analyzing late-season weed spatial distribution patterns in commercial onion fields. *Precision Agriculture, 22*(4), 1317–1332. https://doi.org/10.1007/s11119-021-09786-y

Sellers, B., Rana, N., & Dias, J. L. C. S. (2018). *Smutgrass control in perennial grass pastures*. Gainesville, FL, USA: University of Florida, Florida Cooperative Extension Service. SS-AGR-18

Tamouridou, A. A., Alexandridis, T. K., Pantazi, X. E., Lagopodi, A. L., Kashefi, J., & Moshou, D. (2017). Evaluation of UAV imagery for mapping *Silybum marianum* weed patches. *International Journal of Remote Sensing, 38*(8–10), 2246–2259. https://doi.org/10.1080/01431161.2016.1252475

Wilder, B. J., Sellers, B. A., Ferrell, J. A., & MacDonald, G. E. (2011). Response of smutgrass varieties to hexazinone. *Forage & Grazinglands, 9*(1), 1–7. https://doi.org/10.1094/FG-2011-0222-02-RS

Wunderlin, R. P., & Hansen, B. F. (2003). *Guide to the vascular plants of Florida* (2nd ed.). Florida, USA: University Press of Florida.

Xiang, H., & Tian, L. (2011). Development of a low-cost agricultural remote sensing system based on an autonomous unmanned aerial vehicle (UAV). *Biosystems Engineering, 108*(2), 174–190. https://doi.org/10.1016/j.biosystemseng.2010.11.010

Yuba, N., Kawamura, K., Yasuda, T., Lim, J., Yoshitoshi, R., Watanabe, N., et al. (2021). Discriminating *Pennisetum alopecuoides* plants in a grazed pasture from unmanned aerial vehicles using object-based image analysis and random forest classifier. *Grassland Science, 67*(1), 73–82. https://doi.org/10.1111/grs.12288

Zisi, T., Alexandridis, T., Kaplanis, S., Navrozidis, I., Tamouridou, A.-A., Lagopodi, A., et al. (2018). incorporating surface elevation information in UAV multispectral images for mapping weed patches. *Journal of Imaging, 4*(11), 132. https://doi.org/10.3390/jimaging4110132

Zvoleff, A. (2020). *glcm: Calculate textures from grey-level co-occurrence matrices (GLCMs)*. Retrieved July 24, 2021, from https://CRAN.R-project.org/package=glcm.

Publisher's Note Springer Nature remains neutral with regard to jurisdictional claims in published maps and institutional affiliations.

Authors and Affiliations

Gal Rozenberg[1,2] · José Luiz C. S. Dias[3] · Wesley M. Anderson[4] · Brent A. Sellers[5] · Raoul K. Boughton[6] · Matheus B. Piccolo[7] · Lior Blank[2]

1 Faculty of Civil and Environmental Engineering, Technion-Israel Institute of Technology, Haifa, Israel

2 Department of Plant Pathology and Weed Research, ARO, Volcani Center, Rishon LeZion, Israel

3 School of Plant Sciences, The University of Arizona Cooperative Extension System - Maricopa Agricultural Center, Maricopa, AZ 85138, USA

4 School of Forestry and Wildlife Sciences, Alabama Cooperative Extension System, Auburn University, Auburn, AL 336849, USA

5 Range Cattle Research and Education Center, University of Florida Institute of Food and Agricultural Sciences, Ona, FL, USA

6 The Mosaic Company, Lithia, FL 32259, USA

7 Select Sires Do Brasil, Porto Alegre, RS 91030230, Brazil